**Geoscientific
Model Development
Discussions**

Evaluation of a present-day climate simulation with a new coupled atmosphere-ocean model GENMOM

J. R. Alder[1], **S. W. Hostetler**[2], **D. Pollard**[3], **and A. Schmittner**[4]

[1]Oregon State Univ., Dept. of Geosciences, Corvallis, OR 97331, USA
[2]US Geological Survey, Oregon State Univ., Dept. of Geosciences, Corvallis, OR 97331, USA
[3]Pennsylvania State Univ., EMS Earth and Environmental Systems Institute, University Park, PA 16802, USA
[4]Oregon State Univ., College of Ocean and Atmospheric Sciences, Corvallis, OR 97331, USA

Correspondence to: J. R. Alder (jay.alder@geo.oregonstate.edu)

Discussion Paper | Discussion Paper | Discussion Paper | Discussion Paper

GMDD

3, 1697–1735, 2010

Evaluation of a present-day climate simulation

J. R. Alder et al.

Title Page

Abstract	Introduction
Conclusions	References
Tables	Figures

|◄ | ►|
◄ | ►
Back | Close

Full Screen / Esc

Printer-friendly Version

Interactive Discussion

Abstract

We present a new, non-flux corrected AOGCM, GENMOM, that combines the GENE-SIS version 3 atmospheric GCM (Global ENvironmental and Ecological Simulation of Interactive Systems) and MOM2 (Modular Ocean Model version 2). We evaluate GEN-MOM by comparison with reanalysis products (e.g., NCEP2) and eight models used in the IPCC AR4 assessment. The overall present-day climate simulated by GENMOM is on par with the models used in IPCC AR4. The model produces a global temperature bias of 0.6 °C. Atmospheric features such as the jet stream structure and major semi-permanent sea level pressure centers are well simulated as is the mean planetary-scale wind structure that is needed to produce the correct position of stormtracks. The gradients and spatial distributions of annual surface temperature compare well both to observations and to the IPCC AR4 models. A warm bias of ∼2 °C is simulated by MOM between 200–1000 m in the ocean. Most ocean surface currents are reproduced except where they are not resolved well by the T31 resolution. The two main weak-nesses in the simulations is the development of a split ITCZ and weaker-than-observed overturning circulation.

1 Introduction

We present a new non-flux corrected coupled atmosphere-ocean general circulation model (AOGCM), GENMOM, which combines GENESIS version 3 (Global ENviron-mental and Ecological Simulation of Interactive Systems) and MOM2 (Modular Ocean Model version 2) general circulation models. Both models have been used widely in climate studies that demonstrate their overall ability to produce climate simulations that are in agreement both with observations and with similar models. GENESIS version 1 was developed starting in 1989 at the National Center for Atmospheric Research (NCAR) with a focus on linking terrestrial physical and biophysical processes with the atmosphere to provide a model that could be applied to investigate paleoclimate and possible future climates under global warming.

GENESIS version 1 was released in 1991 (Thompson and Pollard, 1995) and included a land-surface transfer model (LSX) and an atmospheric general circulation model derived from NCAR CCM1. GENESIS version 2 was released in 1995 and included many improvements ranging from new prognostic cloud amounts, the use of
5 hybrid vertical coordinates, the inclusion of gravity wave drag, and to improvements in LSX (Thompson and Pollard, 1997; Pollard and Thompson, 1997).

GENESIS version 3 expands on version 2 by including the NCAR CCM3 radiation code and the ocean can optionally be represented by the MOM2 ocean general circulation model in addition to fixed sea surface temperatures or the slab ocean. MOM also
10 has a long history of use and development spanning back to the early 1990s and is used as the ocean component in many other AOGCMs (Pacanowski, 1996). Our current version of GENMOM uses T31 (~3.75° × 3.75° latitude and longitude) horizontal resolution for both the atmosphere and ocean to balance computational requirements needed for long simulations with the ability to simulate important features of the general
15 circulation.

We evaluate a simulation of modern climate against observations and other coupled AOGCMS. The evaluation demonstrates that GENMOM produces a realistic simulation of modern climate that is on par with that of the models used in the Intergovernmental Panel of Climate Change (IPCC) Forth Assessment Report (AR4). For additional
20 evaluation, we compare GENMOM to eight models evaluated in the World Climate Research Programme's (WCRP's) Coupled Model Intercomparison Project phase 3 (CMIP3, Meehl et al., 2007a), a multi-model dataset that was subsequently used in the IPCC AR4 (described in Table 1, Randall et al., 2007). A full description of GENESIS and MOM2 as well as their coupling is provided in Sect. 2, atmospheric and oceanic
25 results from a modern climate simulation are presented in Sect. 3, and concluding remarks follow in Sect. 4.

Discussion Paper | Discussion Paper | Discussion Paper | Discussion Paper

2 GENMOM description

2.1 GENESIS description

GENESIS has been developed with emphasis on terrestrial physical and biophysical processes, and suitability for paleoclimatic experiments. Earlier versions of GENE-
SIS are described by Thompson and Pollard (1995, 1997) and Pollard and Thompson (1994, 1995, 1997), and have been applied and tested in a wide range of modern and paleoclimate applications including the Paleoclimate Modeling Intercomparison Project (e.g., Pollard et al., 1998; Joussaume et al., 1999; Pinot et al., 1999; Beckmann et al., 2005; Miller et al., 2005; Ruddiman et al., 2005; Bice et al., 2006; DeConto et al., 2006, 2008; Hostetler et al., 2006; Poulsen et al., 2006, 2007; Horton et al., 2007).

The nominal GENESIS resolution is spectral T31 ($3.75° \times 3.75°$) with 18 vertical sigma coordinate levels, 4 of which are above the tropopause. Spectral transform dynamics are used for mass, heat and momentum (Williamson et al., 1987). A semi-Lagrangian transport in grid space is used for water vapor (Williamson and Rasch, 1989). Convection in the free atmosphere and in the planetary boundary layer is treated using an explicit sub-grid buoyant plume model similar to, but simpler than, Kreitzberg and Perkey (1976) and Anthes (1977, Sect. 4). Stratus, convective and anvil cirrus clouds are predicted using prognostic 3-D water cloud amounts, (Smith, 1990; Senior and Mitchell, 1993) and clouds are advected by semi-Lagrangian transport and mixed vertically by convective plumes and background diffusion.

The land-surface transfer model, LSX, accounts for the physical effects of vegetation (Pollard and Thompson, 1995). Up to two vegetation layers (trees and grass) can be specified at each grid point, and the radiative and turbulent fluxes through these layers to the soil or snow surface are calculated. A six-layer soil model extends from the surface to 4.25 m depth, with layer thicknesses increasing from 5 cm at the top to 2.5 m at the bottom. Physical processes in the vertical soil column include heat diffusion, liquid water transport (Clapp and Hornberger, 1978; Dickinson, 1984), surface runoff and bottom drainage, uptake of liquid water by plant roots for transpiration, and the

freezing and thawing of soil ice. A three-layer snow model, which includes fractional area cover when the snow is thin, is used for snow cover on soil, ice-sheet and sea-ice surfaces. A three-layer sea-ice model accounts for local melting, freezing, fractional sea-ice cover (Semtner, 1976; Harvey, 1988), and includes dynamics associated with wind and ocean current using the cavitating-fluid model of Flato and Hibler (1992). Version 3 of GENESIS (Zhou et al., 2008; Kump and Pollard, 2008) incorporates the NCAR CCM3 radiation code (Kiehl et al., 1998) and the ocean is represented by the MOM2 ocean general circulation model (Pacanowski, 1996).

2.2 MOM2 description

MOM2 was developed by the Geophysical Fluid Dynamics Laboratory (GFDL) in the early 1990s, but builds off previous work that began back in 1969 (Pacanowski, 1996). MOM2 is a finite difference implementation of the primitive equations of ocean circulation based on the Navier-Stokes equations with the Boussinesq, hydrostatic, and rigid lid approximations (Bryan, 1969). The Boussinesq approximation invokes constant density with depth, with the exception of terms that contain gravity, thereby reducing computational complexity. The hydrostatic approximation assumes that vertical pressure gradients are density driven. A nonlinear equation of state couples temperature and salinity to fluid velocity. An insulated lateral boundary is used such that no temperature or salinity flux is exchanged between ocean and land cells. Unlike the sigma levels used for atmospheric altitude in GENESIS, MOM uses a fixed z-axis for depth, which simplifies the equations used in the finite difference representation. Our version of MOM2 uses 20 unevenly spaced vertical levels that become progressively thicker with depth, so that the uppermost ocean layers are well resolved. The topmost level is 25 m thick, while the bottommost level is ∼660 m thick. A horizontal resolution of $3.75° \times 3.75°$ is used to match the atmospheric T31 resolution. The hybrid mixing scheme isopycmix is used with a vertical viscosity coefficient of $0.1\,\mathrm{cm^2\,s^{-1}}$ and a vertical diffusion coefficient of $0.35\,\mathrm{cm^2\,s^{-1}}$. Although the Gent-McWilliams mixing scheme is available in MOM2, it was not used in this study.

Full Screen / Esc

Printer-friendly Version

Interactive Discussion

2.3   GENMOM coupling

To simplify the coupling between the atmosphere and ocean, both the GCMs are implemented on essentially the same T31 grid. In MOM2, the latitudinal grid spacing is not exactly T31, but is adjusted with a cosine-stretching factor (Pacanowski, 1996)
5   to closely approximate T31. GENESIS has a 30-min timestep, and MOM2 has a 6 h timestep for scalar fields. The two models interact in an essentially synchronous manner, communicating every 6 h. 6 h averages of the surface fluxes of heat, water and momentum are passed from GENESIS to MOM2, and MOM2 is run through one 6 h scalar timestep. The updated SSTs are passed back to GENESIS and used to run
10 it for the next 6 h. Sea ice is treated within the LSX module of GENESIS, and under sea ice, fluxes between the sea-ice base and the uppermost ocean layer are passed to MOM2. Continental freshwater river runoff is globally averaged and spread over the world ocean.

3   Simulation of the present climate

15 We analyze the annual and seasonal climatologies of the last 30 years of a 700-year control simulation produced by GENMOM. Where possible, we compare the GENMOM results to ensembles of the AOGCMs used in the IPCC AR4 (Randall et al., 2007). We use the last 30 years of the Climate of the 20th Century experiment from eight selected IPCC AR4 models (Table 1) to provide context for evaluating the performance of
20 GENMOM. For the present-day GENMOM simulation, atmospheric CO_2 concentration is prescribed at a constant 355 ppmV, near the mean value for our climatology period of 1981–2005. GENMOM was initialized with a latitudinal-dependent temperature profile while salinity was uniformly prescribed at 35 ppt. Analysis of ocean temperatures indicates that spin up of the model was suitably achieved after 400 years. Over the
25 last century of the simulation the deep ocean (>1000 m) warmed by ~0.002 °C/decade whereas the mid layer (200 m–1000 m) warmed by ~0.003 °C/decade and the surface layer was free of drift.

3.1 Validation datasets and input files

In contrast to the IPCC AR4, wherein a variety of observed datasets are used to evaluate model performance, whenever possible we rely solely on the NOAA NCEP Reanalysis 2 data set (NCEP2, Kanamitsu, et al., 2002) to maintain consistency between and among variable fields. We use a standard climatology period of 1981–2005 for the NCEP2 data unless otherwise specified. Observed SST data are derived from the NOAA Optimum Interpolation Sea Surface Temperature V2 (OI SST, Reynolds, et al., 2002), which is a $1° \times 1°$ gridded dataset based on combining in situ measurements and satellite observations. We use a climatology period of 1982–2005 for OI SST, because 1982 is the first full year for which the data are available. Global subsurface ocean temperatures were obtained from The World Ocean Atlas 2005 (WOA05, Locarnini et al., 2006), which is also a $1° \times 1°$ gridded dataset of ocean temperature and salinity at specific depths. We use the Hadley Ice and Sea Surface Temperature v1.1 (HadISST, UK Meteorological Office, 2006) for observed sea-ice extent data. Finally, to evaluate ocean surface currents and overturning, we use the German partner of the Estimating the Circulation and Climate of the Ocean dataset (GECCO), which is a 50-year (1950–2000) oceanography reanalysis product forced with the first NCEP Reanalysis data (Köhl and Stammer, 2008; NCEP1; Kalnay et al., 1996).

GENMOM input files for topography, bathymetry, and land-ocean mask were derived by interpolating the ICE-4G model (Peltier, 2002) reconstruction from $1° \times 1°$ to T31 resolution. Ice-sheet cover and thickness is prescribed by interpolating the ICE-4G model reconstruction to T31. To maintain numerical stability, over the northernmost Arctic Ocean cells in MOM2 we smooth the bathymetry field derived from ICE-4G with a 9-cell moving window. At T31 horizontal resolution the Bering Strait is closed. Modern values for the distribution of vegetation (Dorman and Sellers, 1989), soil texture (Webb et al., 1993) and freshwater lakes (Cogley, 1991) are prescribed. The use of ICE-4G orography to derive global topography, bathymetry, and ice-sheet extent is based on our goal of streamlining the configuration of GENMOM for paleoclimate applications.

3.2 Atmospheric fields

Overall, the distribution of the zonally averaged profile of air temperature simulated by GENMOM is in agreement with the NCEP2 profile (Fig. 1); however, some deficiencies deserve additional attention. GENMOM simulates a cold bias raging up to 6 °C north of 30° N in the Northern Hemisphere (NH) during both winter and summer, whereas a cold bias south of 60° S in The Southern Hemisphere (SH) is present during austral summer. A cold bias is present in the simulated temperature in the uppermost atmosphere above the wintertime pole. Seasonally, GENMOM simulates the meridional shift of peak insolation and warmest surface temperatures well when compared to observations. The modeled tropical warm region is slightly more compressed meridionally than the NCEP2 data.

The summer and winter patterns and magnitudes of the annually averaged planetary jet stream structure are well captured by GENMOM (Fig. 2). In both winter hemispheres the core of the jetstream (at ~200 hPa) and related upper level winds (500 hPa) are slightly enhanced relative to the NCEP2 data. These minor mismatches notwithstanding, the overall structure of the simulated jetstream suggests that GEN-MOM produces a realistic mean planetary-scale wind structure that is essential to the related positioning of the stormtracks.

GENMOM simulates the seasonally persistent positions of planetary ridges and troughs and thus the upper atmospheric flow and 500 hPa geopotential (Fig. 3a–d). During boreal winter, the ridge over western North America is shifted eastward in GENMOM relative to observations and the associated trough to the east over northern Canada and the North Atlantic is similarly slightly displaced and more zonal relative to that of the NCEP2 data (Fig. 3b). The 500 hPa heights over North America and Eurasia are lower than those of the NCEP2 data resulting in slightly reduced wind velocities, particularly over eastern North America and the North Atlantic. In the SH, austral summer 500 hPa heights are well simulated but wind velocities associated with the westerlies are somewhat reduced due to the lower pressure gradient over

the Southern Ocean and Antarctica and the lack of actual topographic forcing due to smoothing in the model.

During boreal summer, the ridge over western North America is correctly placed in GENMOM, but the amplitude of the ridge is greater than observed and the related downstream trough is slightly deeper than that of the NCEP2 data (Fig. 3c). Heights in the region extending east of the Mediterranean and across India and China appear modestly lower than observed; however, part of the apparent discrepancy stems from values that are just above or just below the color breaks in the plotting scales.

In the SH, the comparison for the austral winter is similar to that of the austral summer. Spatial patterns of winter and summer mean sea level pressure (MSLP) are captured by GENMOM; however, regional differences exist (Fig. 3e–h). During boreal winter GENMOM simulates lower-than-observed MSLP in the Aleutian and Icelandic lows. As a result, wind velocities are enhanced over North America. In the SH, surface pressure and winds are comparable with those of the NCEP2 data except along SH westerlies where MSLP is higher and wind velocities are lower due to the reduced pressure gradient.

The boreal summer simulation of MSLP and wind velocities is quite good; the subtropical highs in the NH are well placed and the associated wind velocities are comparable to NCEP2 (Fig. 3h). MSLP and wind velocities in the tropics and the SH are also well simulated by GENMOM. During austral summer, the SH high-pressure anticyclones are somewhat weaker than observed. The simulated south Pacific high is weak and so does not produce anticyclonic flow, which contributes to a weakened South Pacific Gyre. The SH westerly winds are simulated to be too weak, presumably due to coarse resolution topography, which will influence ocean overturning. GENMOM simulates stronger-than-observed westerly winds across southern Europe, which is caused by the overactive Icelandic low. This is likely due to a cold temperature bias in the Norwegian Sea, which fails to isolate the low pressure center.

The vertical profile of atmospheric specific humidity simulated by GENMOM is in agreement with the NCEP2 data (Fig. 4). A dry bias, evident over the tropics, and

Evaluation of a present-day climate simulation

J. R. Alder et al.

Title Page

Abstract | Introduction

Conclusions | References

Tables | Figures

⏮ | ⏭

◀ | ▶

Back | Close

Full Screen / Esc

Printer-friendly Version

Interactive Discussion

a wet bias, evident in the SH below 700 hPa, are associated with the warm bias in atmospheric temperature caused by a warm Southern Ocean. A wet bias over the NH below 700 hPa is not associated with a warm bias in atmospheric temperature; rather, it is caused by weak convection from the surface to ∼400 hPa between 70° N–80° N.

3.3 Modeled surface temperatures

The simulated global mean-annual 2 m air temperature is 278.3 K, in good agreement with the NCEP2 value of 278.9 K (Fig. 5). Over land the simulated temperature is 1.3 K colder than observed and over the oceans simulated temperature is 0.6 K warmer than observed. GENMOM simulates the meridional temperature gradient well. Major topographic features resolved by the model such as the Rocky Mountains, the Andes and the Himalayas, have regional temperatures that match well to observation. We note that the high latitude temperature anomalies (Fig. 6) are partially attributed to a mismatch between the ICE-4G derived land mask and that of NOAA OI SST V2 interpolated to T31. Where a mismatch occurs, large anomalies are created due to comparing an SST grid cell to a 2 m air temperature grid cell.

Exceptions to the agreement between simulated and observed 2 m temperatures are primarily found over the oceans (Figs. 5 and 6). The Southern Ocean warm bias may be caused by weaker-than-observed westerly winds across the Southern Ocean resulting in weak ocean overturning. The cold bias over the Norwegian Sea is caused by too much simulated sea-ice, as a result of too weak meridional overturning. Because the cold water tongue associated with the California Current is ∼300 km wide, it is not adequately resolved at T31, and leads to a warm bias along the Pacific coast of North America. The northward branch of the South Pacific Gyre also is not well resolved in addition to weak westerly trade winds, resulting in a weak cold water Humboldt Current along the western coast of South America. The weakened circulation results in a warm SST bias off the coast of Chile.

Our GENMOM simulation has many features in common with the IPCC AR4 models, including: (1) a cold bias over northern Europe, (2) a warm SST bias in the waters

west of South America, (3) a warm bias in the Southern Ocean and (4) cold biases over the Himalayas and Greenland (Fig. 6). In contrast to many of the IPCC AR4 models, GENMOM simulates the annual surface temperature over much of Antarctica with anomalies <2 °C.

5 GENMOM captures the global patterns of the seasonal cycle of temperature but overestimates the amplitude over Greenland, South America, southeast United States and Australia and underestimates the amplitude over northern Africa, the western United States and much of Europe and Asia (Fig. 7). The model also simulates greater variability over some of the oceans, particularly in the mid latitudes. Similar to Fig. 6,

10 grid cells where the land-ocean distribution does not match have large seasonal cycle amplitude anomalies.

3.4 Precipitation

GENMOM simulates global mean-annual precipitation reasonably well relative to both the reanalysis data and the IPCC models (Figs. 8, 9). Similar to other AOGCMs, GEN-

15 MOM produces a split Intertropical Convergence Zone (ITCZ) in the tropical Pacific. During DJF, the southern branch of the ITCZ simulated by GENMOM extends too far to the east. In JJA, the northern branch of the ITCZ simulated by GENMOM is compressed and extends too far to the north relative to observations. Lin (2007) found that many IPCC AR4 models produce a double ITCZ which is caused by: (1) excessive

20 tropical precipitation, (2) high sensitivity of modeled precipitation and surface air humidity to SST, (3) a lack of sensitivity of cloud amount to precipitation, and (4) a lack of sensitivity of stratus cloud formation to SST. GENMOM produces a cold SST bias in the Pacific Basin along with a confined cold tongue, both of which Lin (2007) noted as factors that result in a double ITCZ. Consistent with Lin (2007), GENMOM does

25 not produce a significant double ITCZ when coupled to a slab ocean due to weakened ocean-atmosphere feedbacks. The double ITCZ problem can potentially be resolved by improving these ocean-atmosphere feedbacks.

Full Screen / Esc

Printer-friendly Version

Interactive Discussion

Globally, GENMOM underestimates seasonal DJF precipitation in the Indian Ocean and JJA precipitation over the southern Asian landmass and Atlantic precipitation. The zonally averaged annual precipitation clearly illustrates the double ITCZ in GENMOM (Fig. 10); the double peak in total precipitation is evident at 10° N and 10° S rather than

5 the observed single and stronger peak between 10° N and 0° N. Outside of the tropics however, the modeled precipitation compares well with reanalysis and the selected IPCC AR4 model simulations.

3.5 Oceanic fields

The overall patterns of surface and subsurface ocean temperatures simulated by GEN-

10 MOM compare well to observations; however, anomalies reveal biases exceeding 2 °C (Fig. 11). A cold bias is simulated over much of the surface and a warm bias is simulated in around the thermocline in the tropics. A warm bias in the near-surface of the Southern Ocean is consistent with the surface temperature anomalies shown in Fig. 6. The Southern Ocean warm bias is likely caused by weak ocean overturning. The warm

15 bias in the tropical ocean mid-depths is attributed to weakened simulated upwelling and the use of a relatively high vertical diffusion coefficient ($0.35 \, \text{cm}^2 \, \text{s}^{-1}$) that is prescribed to maintain reasonable ocean overturning; too much heat is diffused from the surface to the mid-depths.

GENMOM captures the observed zonal distribution of salinity well for the Atlantic

20 Ocean and Indian + Pacific Oceans with a few region specific discrepancies (Fig. 12). Relative to the WOA05 data, in the Atlantic, GENMOM simulates lower salinity waters at high latitudes and higher salinity waters in the northern mid latitudes; the maximum centered on 30° N exceeds observations and the maximum at 30° S underestimates observations. A 1+ PSS salinity bias in the northern mid latitudes between 400–1000 m

25 is attributed to a build up of salinity in the Gulf of Mexico caused by weaker-than-observed circulation associated with the coarse resolution of ocean orography. Similarly, the low salinity bias north of 60° N is associated with reduced northward penetration of the North Atlantic Drift into the Arctic, again due to the coarse resolution of

Full Screen / Esc

Printer-friendly Version

Interactive Discussion

ocean orography, and weaker-than-observed Atlantic Meridional Overturning Circulation (AMOC). GENMOM does a good job at simulating the difference in salinity between the Atlantic Ocean and Indian + Pacific Oceans. Salinity in the Indian + Pacific Oceans matches well to observations with much of the zonal bias being less than ±0.2 PSS.

⁵ We compare simulated global and basin ocean overturning for the full 300-year GEN-MOM with observations (Fig. 13). The last 30 years of the simulation coincidently displayed one of the weakest periods of overturning in the 300-yr simulation, so we use the full 300-year record as more representative in that multidecadal variability is smoothed out in the average. Globally, GENMOM simulates an overturning similar in pattern to
¹⁰ that of the GECCO data. The most notable shortcoming in the GENMOM simulation is that the strength and depth of the Deacon Cell, which is characterized as deep clockwise meridional circulation in the Southern Ocean driven by windstress, are poorly captured. Wind velocities across the Southern Ocean are weaker-than-observed (Fig. 3) thereby failing to produce sufficient windstress to drive deep overturning (Toggweiler
¹⁵ and Samuels, 1995; Sijp and England, 2009). The weak westerly winds are likely due to the coarse meridional resolution (Held and Phillipps, 1993; Tibaldi et al., 1990) and may also contribute to weak AMOC biases in non-flux corrected models with coarse atmospheric resolution, as found in earlier studies (Bryan et al., 2006; Schmittner et al., 2010). GENMOM's failure to simulate the Deacon Cell contributes to the warm
²⁰ Southern Ocean temperature bias by not upwelling deep cold water.

The simulated AMOC is similar in pattern to that of the GECCO data but it is somewhat weaker in strength. The maximum AMOC strength over the 300-year simulation is 13.3 ± 0.8 Sv, which is lower than the observed 16–18 Sv range. The models used in the IPCC AR4 generally fall between 12–20 Sv (Meehl et al., 2007b; Schmittner et
²⁵ al., 2005). The combined Indian Ocean and Pacific Ocean overturning matches well with observations with the exception that GENMOM simulates deeper-than-observed clockwise overturning in the northern tropics, which may imply the vertical diffusion coefficient is too high.

Printer-friendly Version

Interactive Discussion

GENMOM produces ocean surface currents that match generally well to observations on an annual average (Fig. 14). The major Atlantic surface currents are well simulated in GENMOM, with the exception of the Gulf Stream, which is too weak. The Antarctic Circumpolar Current flowing through the Drake Passage is well resolved, as is the continuing flow to the South Atlantic Current. In the Pacific, the equatorial currents are well simulated, but the North Equatorial Counter Current is not present and the North Equatorial Current weaker than that of the observations. The Kuroshio Current is well placed but also slightly weaker than that of the observations. The California Current is noticeably absent from the GENMOM simulated surface currents. Both the Humboldt Current and Antarctic Circumpolar Current have weaker-than-observed strengths. The strength of the Antarctic Circumpolar Current through the Drake Passage is simulated to be 35% weaker than the 119 Sv found in the GECCO reanalysis. In the Indian Ocean, GENMOM simulates the Indonesian Throughflow realistically, matching observations well. The Indonesian Throughflow throughput is found to be 12.7 ± 0.8 Sv, which compares well to the observed estimates of 9.3 ± 2.5 Sv (Gordon et al., 1999) and 13.2 ± 1.8 Sv (Lumpkin and Speer, 2007). Surface currents in the northern Indian Ocean are modulated by the monsoon, where currents flow westward during winter and eastward during summer. The annually averaged surface currents in Fig. 14 show westward flow dominating in GENMOM whereas eastward flow dominates in the observations. The incorrect direction of surface currents is most noticeable in GENMOM during winter and spring. Most of the deficiencies in simulated surface currents are attributed to the coarse resolution of the model and related inability to resolve subgrid components of the current.

GENMOM simulates winter sea-ice extent and concentration well in the NH for both DJF and JJA (Fig. 15). Sea-ice extends too far into the Norwegian Sea during both winter and summer and too far into Hudson Bay during winter. The excessive sea-ice in the Norwegian Sea is likely due to a weak AMOC, which is not transporting enough warm mid-latitude water north. Antarctica shows deficient sea-ice during both seasons, which may be explained by the warm temperature bias in the Southern Ocean.

Antarctic winter sea-ice fails to reach the full extent seen in the observed dataset due to the warm SST bias in the Southern Ocean.

4 Conclusions

We present the first formal evaluation of the new AOGCM GENMOM, which is a non-flux corrected model comprised of GENESIS 3 atmospheric model, MOM2 ocean model and LSX. The main changes in GENESIS version 3 are (i) solar and thermal infrared radiation are calculated using the NCAR CCM3 radiation code, and (ii) the ocean is represented by the MOM2 ocean general circulation model. The spectral resolution of T31 for both atmosphere and ocean is used during this evaluation.

The simulated global 2 m air temperature is 0.6 °C warmer over oceans and 1.3 °C colder over land. The jet stream structure and major planetary features of sea level pressure are well captured by the model. GENMOM produces a realistic mean planetary-scale wind structure that is needed to produce the correct position of storm-tracks. The 500 hPa ridges and troughs are well simulated, as are the seasonal surface pressure cyclones and anticyclones.

The annual surface temperature gradient and spatial distribution compare well both to observations and to the IPCC AR4 models. Cold SST anomalies in the Norwegian Sea are explained by excessive sea-ice in both winter and summer, which is in turn caused by weak Atlantic Ocean overturning. A warm bias in the Southern Ocean is attributed to a weak ocean overturning resulting in a poor simulation of the Deacon Cell, which suppresses associated cold water upwelling in the Southern Ocean. GENMOM fails to resolve adequately the South Pacific Gyre, which results in a warm SST bias in the eastern Pacific Ocean and weak anticyclonic atmospheric circulation around the gyre. GENMOM simulates a double ITCZ when coupled with the OGCM, which is not present when GENESIS is coupled to a slab ocean.

The global ocean temperature is generally well simulated, with the exception of a warm bias between 200–1000 m in the tropics and mid-latitudes. The warm bias is

Full Screen / Esc

Printer-friendly Version

Interactive Discussion

attributed to weak global overturning and the use of a high value of the vertical diffusion coefficient, which was needed to maintain realistic global ocean overturning. Salinity is generally well simulated, but with a fresh bias in the North Atlantic caused by underrepresentation of narrow channels (i.e., the Norwegian Sea) at T31 model resolution and a 1+ PSS salinity bias in the northern mid latitudes originating in the Gulf of Mexico. Ocean overturning is simulated with the correct spatial pattern, but is generally weaker-than-observed. We attribute the weak meridional ocean overturning to (i) weak and northwardly displaced westerly winds in the SH due to coarse topography and (ii) a narrow and shallow Drake Passage also due to coarse orography.

Most ocean surface currents are well simulated by GENMOM, with the exception of narrow currents such as the Gulf Stream and the Kuroshio Current that are weaker-than-observed again due to the coarse T31 resolution. Northern Hemisphere Sea-ice is well simulated with the exception of excess sea-ice in the Norwegian Sea. However, the SH sea-ice extent is too small compared to observations. Both NH and SH deficiencies are linked to weak ocean overturning.

The evaluation performed here has shown that GENMOM produces a realistic climatology that is comparable to the models used in the IPCC AR4. GENMOM shares similar deficiencies with other models such as a double ITCZ, failure to resolve features due to resolution limitations (the California and Humboldt Currents), weak ocean overturning and having a general global cold bias. Despite these deficiencies, GENMOM produces biases that are within the range seen in the IPCC models. The overall climatology simulated by GENMOM is generally similar to that of previous GENESIS versions. The addition of a coupled ocean model, however, allows GENMOM to be used in studying phenomena such as ENSO that require dynamic ocean-atmosphere interaction.

References

Anthes, R. A.: A cumulus parameterization scheme utilizing a one-dimensional cloud model, Mon. Weather Rev., 105, 270–286, 1977.

Beckmann, B., Floegel, S., Hoffman, P., Schulz, M., and Wagner, T.: Orbital forcing of Cretaceous river discharge in tropical Africa and ocean response, Nature, 437, 241–244, 2005.

Bice, K. L., Birgel, D., Meyers, P. A., Dahl, K. A., Hinrichs, K. U., and Norris, R. D.: A multiple proxy and model study of Cretaceous upper ocean temperatures and atmospheric CO_2 concentrations, Palaeoceanography, 21, PA2002, doi:10.1029/2005PA001203, 1–17, 2006.

Bryan, F. O., Danabasoglu, G., Nakashiki, N., Yoshida, Y., Kim, D. H., Tsutsui, J., and Doney, S. C.: Response of the North Atlantic thermohaline circulation and ventilation to increasing carbon dioxide in CCSM3, J. Climate, 19, 2382–2397, 2006.

Bryan, K.: A numerical method for the study of the circulation of the world oceans, J. Comput. Phys., 4, 347–376, 1969.

Clapp, R. B. and Hornberger, G. M.: Empirical equations for some soil hydraulic properties, Water Res. Res., 14, 601–604, 1978.

Cogley, J. G.: GGHYDRO–Global hydrological data release 2.0, Trent Clim. Note 91-1, 13 pp., Dep. Geogr., Trent Univ., Peterborough, Ont, 1991.

Collins, W. D., Rasch, P. J., Boville, B. A., McCaa, J. R., Williamson, D. L., Kiehl, J. T., Briegleb, B., Bitz, C., Lin, S.-J., Zhang, M., and Dai, Y.: Description of the NCAR Community Atmosphere Model (CAM3.0), Technical Note TN-464+STR, National Center for Atmospheric Research, Boulder, Colo., 214 pp., 2004.

DeConto, R. M., Pollard, D., and Harwood, D.: Sea ice feedback and Cenozoic evolution of Antarctic climate and ice sheets, Paleoceanography, 22, PA3214, doi:10.1029/2006PA001350, 2006.

DeConto, R. M., Pollard, D., Wilson, P., Palike, H., Lear, C., and Pagani, M.: Thresholds for Cenozoic bipolar glaciation, Nature, 455, 653–656, 2008.

Dickinson, R. E.: Modeling evapotranspiration for three-dimensional global climate models,

⏮ | ⏭

◀ | ▶

Back | Close

Full Screen / Esc

Printer-friendly Version

Interactive Discussion

in: Climate Processes and Climate Sensitivity, edited by: Hansen, J. E. and Takahashi, T., Geophys. Monograph, 29, American Geophysical Union, Washington DC, 58–72, 1984.

Dorman, J. L. and Sellers, P. J.: A global climatology of albedo, roughness and stomatal resistance for atmospheric general circulation models as represented by the Simple Biosphere Model (SB), J. Appl. Meteor., 28, 833–855, 1989.

Flato, G. M.: The Third Generation Coupled Global Climate Model (CGCM3) (and included links to the description of the AGCM3 atmospheric model). http://www.cccma.bc.ec.gc.ca/models/cgcm3.shtml, 2005.

Flato, G. M. and Hibler, W. D.: Modeling pack ice as a cavitating fluid, J. Phys. Oceanogr., 22, 626–651, 1992.

GFDL GAMDT (The GFDL Global Atmospheric Model Development Team): The new GFDL global atmosphere and land model AM2-LM2: Evaluation with prescribed SST simulations, J. Climate, 17, 4641–4673, 2004.

Gnanadesikan, A., Dixon, K. W., Griffies, S. W., et al.: GFDLs CM2 global coupled climate modelsPart 2: The baseline ocean simulation, J. Climate, 19, 675–697, 2004.

Gordon, A. L., Susanto, R. D., and Ffield, A.: Throughflow within Makassar Strait, Geophys. Res., Lett., 26, 3325–3328, 1999.

Gordon, C., Cooper, C., Senior, C. A., Banks, H., Gregory, J. M., Johns, T. C., Mitchell, J. F. B., and Wood, R. A.: The simulation of SST, sea ice extents and ocean heat transports in a version of the Hadley Centre coupled model without flux adjustments, Clim. Dynam., 16, 147–168, 2000.

Gordon, H. B., Rotstayn, L. D., McGregor, J. L., Dix, M. R., Kowalezyk, E. A., OFarrell, S. P., Waterman, L. J., Hirst, A. C., Wilson, S. G., Collier, M. A., Watterson, I. G., and Elliott, T. I.: The CSIRO Mk3 Climate System Model. CSIRO Atmospheric Research Technical Paper No. 60, Commonwealth Scientific and Industrial Research Organisation Atmospheric Research, Aspendale, Victoria, Australia, 130 pp., http://www.cmar.csiro.au/e-print/open/gordon2002a.pdf, 2002.

Harvey, L. D. D.: Development of a sea ice model for use in zonally averaged energy balance climate models, J. Climate, 1, 1221–1238, 1988.

Held, I. M. and Phillipps, P. J.: Sensitivity of the Eddy Momentum Flux to Meridional Resolution in Atmospheric Gcms, J. Climate, 6, 499–507, 1993.

Horton, D. E., Poulsen, C. J., and Pollard, D.: Orbital and CO_2 forcing of late Paleozoic continental ice sheets, Geophys. Res. Lett., 34, L19708, doi:10.1029/2007GL031188, 2007.

Evaluation of a present-day climate simulation

J. R. Alder et al.

Hostetler, S. W., Pisias, N. J., and Mix, A. C.: Sensitivity of Last Glacial Maximum climate to uncertainties in tropical and subtropical ocean temperatures, Quaternry Sci. Rev., 25, 1168–1185, 2006.

Joussaume, S., Taylor, K. E., Braconnot, P., Mitchell, J. F. B., Kutzbach, J.E., Harrison, S. P., Prentice, I. C., Broccoli, A. J., Abe-Ouchi, A., Bartlein, P. J., Bonfils, C., Dong, B., Guiot, J., Herterich, K., Hewitt, C. D., Jolly, D., Kim, J. W., Kislov, A., Kitoh, A., Loutre, M. F., Masson, V., McAvaney, B., McFarlane, N., de Noblet, N., Peltier, W. R., Peterschmitt, J. Y., Pollard, D., Rind, D., Royer, J. F., Schlesinger, M. E., Syktus, J., Thompson, S., Valdes, P., Vettoretti, G., Webb, R. S., and Wyputta, U.: Monsoon changes for 6000 years ago: Results of 18 simulations from the Paleoclimate Modeling Inter- comparison Project (PMIP), Geophys. Res. Lett., 26, 859–862, 1999.

K-1 Model Developers: K-1 Coupled Model (MIROC) Description. K-1 Technical Report 1 [Hasumi, H., and S. Emori (eds.)]. Center for Climate System Research, University of Tokyo, Tokyo, Japan, 34 pp., http://www.ccsr.u-tokyo.ac.jp/kyosei/hasumi/MIROC/tech-repo.pdf, 2004.

Kalnay, E., Kanamitsu, M., Kistler, R., Collins, W., Deaven, D., Gandin, L., Iredell, M., Saha, S., White, G., Woollen, J., Zhu, Y., Leetmaa, A., Reynolds, B., Chelliah, M., Ebisuzaki, W., Higgins, W., Janowiak, J., Mo, K.C., Ropelewski, C., Wang, J., Jenne, R., and Joseph, D.: The NCEP/NCAR 40-Year Reanalysis Project, B. Am. Meteorol. Soc., 77, 437–471, 1996.

NCEP-DEO AMIP-II Reanalysis (R-2): Kanamitsu, M., Ebisuzaki, W., Woollen, J., Yang, S.-K., Hnilo, J. J., Fiorino, M., and Potter, G .L., Bul. of the Atmos. Met. Soc, 1631–1643, 2002.

Kiehl, J. T., Hack, J. J., Bonan, G. B., Boville, B. A., Williamson, D. L., and Rasch, P. J.: The National Center for Atmospheric Research Community Climate Model: CCM3, J. Climate, 11, 1131–1149, 1998.

Köhl, A. and Stammer, D.: Decadal sea level changes in the 50-year GECCO ocean synthesis, J. Climate, 21, 1876–1890, 2008.

Kreitzberg, C. W. and Perkey, D. J.: Release of potential instability: Part I. A sequential plume model within a hydrostatic primitive equation model. J. Atmos. Sci., 33, 456–475, 1976.

Kump, L. R. and Pollard, D.: Amplification of Cretaceous warmth by biological cloud feedbacks, Science, 320, 195, 2008.

Lin, J. L.: The double-ITCZ problem in IPCC AR4 coupled GCMs: Ocean–atmosphere feedback analysis, J. Climate, 20, 4497–4525, 2007.

Locarnini, R. A., Mishonov, A. V., Antonov, J. I., Boyer, T. P., and Garcia, H. E.: World Ocean At-

Evaluation of a present-day climate simulation

J. R. Alder et al.

las 2005, Volume 1: Temperature. S. Levitus, Ed. NOAA Atlas NESDIS 61, U.S. Government Printing Office, Washington, D.C., 182 pp., 2006.

Lumpkin, R. and Speer, K.: Global ocean meridional overturning, J. Phys., Oceanogr., 37, 2550–2562, 2007.

Marsland, S. J., Haak, H., Jungclaus, J. H., Latif, M., and Röske, F.: The Max- Planck-Institute global ocean/sea ice model with orthogonal curvilinear coordinates. Ocean Modelling, 5, 91–127, 2003.

McFarlane, N. A., Boer, G. J., Blanchet, J.-P., and Lazare, M.: The Canadian Climate Centre second-generation general circulation model and its equilibrium climate, J. Climate, 5, 1013–1044, 1992.

Meehl, G. A., Covey, C., Delworth, T., Latif, M., McAvaney, B., Mitchell, J. F. B., Stouffer, R. J., and Taylor, K. E.: The WCRP CMIP3 multi-model dataset: A new era in climate change research, B. Am. Meteorol. Soc., 88, 1383–1394, 2007a.

Meehl, G. A., Stocker, T. F., Collins, W. D., Friedlingstein, P., Gaye, A. T., Gregory, J. M., Kitoh, A., Knutti, R., Murphy, J. M., Noda, A., Raper, S. C. B., Watterson, I. G., Weaver, A. J., and Zhao, Z.-C.: Global Climate Projections. in: Climate Change 2007: The Physical Science Basis. Contribution of Working Group I to the Fourth Assessment Report of the Intergovernmental Panel on Climate Change, edited by: Solomon, S., Qin, D., Manning, M., Chen, Z., Marquis, M., Averyt, K. B., Tignor, M., and Miller, H. L., Cambridge University Press, Cambridge, UK and New York, NY, USA, 2007b.

Miller, G., Mangan, J., Pollard, D., Thompson, S., Felzer B., and Magee, J.: Sensitivity of the Australian monsoon to insolation and vegetation: implications for human impact on continental moisture balance, Geology, 33, 1, 65–68, 2005.

Pacanowski, R. C., Dixon, K., and Rosati, A.: The GFDL Modular Ocean Model Users Guide, Version 1.0. GFDL Ocean Group Technical Report No. 2, Geophysical Fluid Dynamics Laboratory, Princeton, NJ, 1993.

Pacanowski, R. C.: MOM 2 Version 2.0 (Beta) Documentation: User's Guide and Reference Manual. NOAA GFDL Ocean Technical Report 3.2, 329 pp., 1996.

Peltier, W. R.: Global glacial isostatic adjustment: palaeogeodetic and space-geodetic tests of the ICE-4G (VM2) model, J. Quaternary Sci., 17 491–510, ISSN 0267-8179, 2002.

Pinot, S., Ramstein, G., Harrison, S. P., Prentice, I. C., Guiot, J., Stute, M., and Joussaume, S.: Tropical paleoclimates at the Last Glacial Maximum: Comparison of Paleoclimate Modeling Intercomparison Project (PMIP) simulations and paleodata, Clim. Dynam., 15, 857–874,

Evaluation of a present-day climate simulation

J. R. Alder et al.

1999.

Pollard, D., Bergengren, J. C., Stillwell-Soller, L. M., Felzer, B., and Thompson, S. L.: Climate simulations for 10 000 and 6 000 years BP using the GENESIS global climate model, Paleoclimates – Data and Modelling, 2, 183–218, 1998.

5 Pollard, D. and Thompson, S. L.: Sea-ice dynamics and CO_2 sensitivity in a global climate model, Atmos.-Ocean, 32, 449–467, 1994.

Pollard, D. and Thompson, S. L.: Use of a land-surface-transfer scheme (LSX) in a global climate model (GENESIS): The response to doubling stomatal resistance, Global Planet. Change, 10, 129–161, 1995.

10 Pollard, D. and Thompson, S.L.: Climate and ice-sheet mass balance at the last glacial maximum from the GENESIS version 2 global climate model, Quaternary Sci. Rev., 16, 841–864, 1997.

Pope, V. D., Gallani, M. L., Rowntree, P. R., and Stratton, R. A.: The impact of new physical parametrizations in the Hadley Centre climate model: HadAM3, Clim. Dynam., 16, 123–146,
15 2000.

Poulsen, C. J., Pollard, D., and White, T. S.: General Circulation Model simulation of the d18O content of continental precipitation in the middle Cretaceous: A model-proxy comparison, Geology, 35, 199–202, 2006.

Poulsen, C. J., Pollard, D., Montanez I. P., and Rowley, D.: Late Paleozoic tropical climate
20 response to Gondwanan glaciation, Geology, 35, 771–774, 2007.

Randall, D. A., Wood, R. A., Bony, S., Colman, R., Fichefet, T., Fyfe, J., Kattsov, V., Pitman, A., Shukla, J., Srinivasan, J., Stouffer, R.J., Sumi, A., and Taylor, K. E.: Climate Models and Their Evaluation. In: Climate Change 2007: The Physical Science Basis, in: Contribution of Working Group I to the Fourth Assessment Report of the Intergovernmental Panel on Climate
25 Change edited by: Solomon, S., Qin, D., Manning, M., Chen, Z., Marquis, M., Averyt, K. B., Tignor, M., and Miller, H. L., Cambridge University Press, Cambridge, United Kingdom and New York, NY, USA, 2007.

Reynolds, R. W., Rayner, N. A., Smith, T. M., Stokes, D. C., and Wang, W.: An Improved In Situ and Satellite SST Analysis for Climate, J. Climate, 15, 1609–1625, 2002.

30 Roeckner, E., Arpe, K., Bengtsson, L., Christoph, M., Claussen, M., Dümenil, L., Esch, M., Giorgetta, M., Schlese, U., and Schulzweida, U.: The Atmospheric General Circulation Model ECHAM4: Model Description and Simulation of Present-Day Climate, MPI Report No. 218, Max Planck Institute for Meteorology, Hamburg, Germany, 90 pp., 1996.

Title Page

Abstract | Introduction

Conclusions | References

Tables | Figures

|◄ | ►|

◄ | ►

Back | Close

Full Screen / Esc

Printer-friendly Version

Interactive Discussion

Roeckner, E., Bäuml, G., Bonaventura, L., et al.: The Atmospheric General Circulation Model ECHAM5. Part I: Model Description, MPI Report 349, Max Planck Institute for Meteorology, Hamburg, Germany, 127 pp., 2003.

Ruddiman, W. F., Vavrus, S. J., and Kutzbach, J. E.: A test of the overdue-glaciation hypothesis, Quat. Sci. Rev., 24, 1–10, 2005.

Schmittner, A., Latif, M., and Schneider, B.: Model projections of the North Atlantic thermohaline circulation for the 21st century assessed by observations, Geophys. Res. Lett., 32, L23710, doi:10.1029/2005GL024368, 2005.

Schmittner, A., Silva, T. A. M., Fraedrich, K., Kirk, E., and Lunkeit, F.: Effects of Mountains on Global Ocean Circulation, J. Climate, submitted, 2010.

Semtner, A. J.: A model for the thermodynamic growth of sea ice in numerical investigations of climate, J. Phys. Oceanogr., 6, 379–389, 1976.

Senior, C. A. and Mitchell, J. F. B.: Carbon dioxide and climate: the impact of cloud parameterization, J. Climate, 6, 393–418, 1993.

Sijp, W. P. and England, M. H.: Southern Hemisphere Westerly Wind Control over the Ocean's Thermohaline Circulation, J. Climate, 22, 1277–1286, 2009.

Smith, R. N. B.: A scheme for predicting layer clouds and their water content in a general circulation model, Q. J. Roy. Meteorol. Soc., 116, 435–460, 1990.

Smith, R. D. and Gent, P. R.: Reference Manual for the Parallel Ocean Program (POP), Ocean Component of the Community Climate System Model (CCSM2.0 and 3.0). Technical Report LA-UR-02-2484, Los Alamos National Laboratory, Los Alamos, NM, http://www.ccsm.ucar.edu/models/ccsm3.0/pop/, 2002.

Thompson, S. L. and Pollard, D.: A global climate model (GENESIS) with a land-surface-transfer scheme (LSX). Part 1: Present-day climate, J. Climate, 8, 732–761, 1995.

Thompson, S. L. and Pollard, D.: Greenland and Antarctic mass balances for present and doubled CO2 from the GENESIS version 2 global climate model, J. Climate, 10, 871–900, 1997.

Tibaldi, S., Palmer, T. N. Brankovic, C., and Cubasch, U.: Extended-Range Predictions with ECMWF Models: Influence of Horizontal Resolution on Systematic-Error and Forecast Skill, Q. J. Roy. Meteor. Soc., 116, 835–866, 1990.

Toggweiler, J. R. and Samuels, B.: Effect of Drake Passage on the Global Thermohaline Circulation, Deep Sea Res. I, 42, 477–500, 1995.

UK Meteorological Office, Hadley Centre: HadISST 1.1 - Global sea-Ice coverage and SST

Evaluation of a present-day climate simulation

J. R. Alder et al.

Title Page

Abstract | Introduction

Conclusions | References

Tables | Figures

◀ | ▶

◀ | ▶

Back | Close

Full Screen / Esc

Printer-friendly Version

Interactive Discussion

(1870-Present), [Internet]. British Atmospheric Data Centre, Downloaded 2/8/2010, http://badc.nerc.ac.uk/data/hadisst/, 2006.

Webb, R. S., Rosenzweig, C. E., and Levine, E. R.: Specifying land surface characteristics in general circulation models: Soil profile data set and derived water-holding capacities, Global Biogeochem. Cy., 7, 97–108, 1993.

Williamson, D. L. and Rasch, P. J.: Two-dimensional semi-Lagrangian transport with shape-preserving interpolation, Mon. Weather. Rev., 117, 102–129, 1989.

Williamson, D. L., Kiehl, J. T., Ramanathan, V., Dickinson, R. E., and Hack, J. J.: Description of NCAR Community Climate Model (CCM1). NCAR Technical Note NCAR/TN-285+STR, Boulder, Colorado, 112 pp., 1987.

Wolff, J.-O., Maier-Reimer, E., and Lebutke, S.: The Hamburg Ocean Primitive Equation Model. DKRZ Technical Report No. 13, Deutsches KlimaRechenZentrum, Hamburg, Germany, 100 pp., http://www.mad.zmaw.de/Pingo/reports/ReportNo.13.pdf, 1997.

Zhou, J., Poulsen, C. J., Pollard, D., and White, T. S.: Simulation of modern and middle Cretaceous marine d18O with an ocean-atmosphere general circulation model, Paleoceanography, 23, PA3223, doi:10.1029/2008PA001596, 2008.

Evaluation of a present-day climate simulation

J. R. Alder et al.

Title Page

Abstract | Introduction

Conclusions | References

Tables | Figures

◀ | ▶

◀ | ▶

Back | Close

Full Screen / Esc

Printer-friendly Version

Interactive Discussion

Table 1. Eight AOGCMs used in the IPCC AR4. T indicates the horizontal resolution using spectral truncation. L indicates the number of levels used in the model.

Model	Modeling Center, Country	Atmosphere Resolution	Ocean Resolution
CCCMA CGCM 3.1 T63	Canadian Centre for Climate Modelling and Analysis, Canada	T47 ($\sim 2.8° \times 2.8°$) L31 McFarlane et al., 1992; Flato, 2005	$1.9° \times 1.9°$ L29 Pacanowski et al., 1993
CSIRO MK 3.0	Commonwealth Scientific and Industrial Research Organisation (CSIRO) Atmospheric Research, Australia	T63 ($\sim 1.9° \times 1.9°$) L18 Gordon et al., 2002	$0.8° \times 1.9°$ L31 Gordon et al., 2002
GFDL CM 2.0	US Department of Commerce/National Oceanic and Atmospheric Administration (NOAA)/Geophysical Fluid Dynamics Laboratory (GFDL), USA	$2.0° \times 2.5°$ L24 GFDL GAMDT, 2004	$0.3° - 1.0° \times 1.0°$ Gnanadesikan et al., 2004
MIROC 3.2 medres	Center for Climate System Research (University of Tokyo) National Institute for, Environmental Studies, and Frontier Research Center for Global Change (JAMSTEC), Japan	T42 ($\sim 2.8° \times 2.8°$) L20 K-1 Developers, 2004	$0.5° - 1.4° \times 1.4°$ L43 K-1 Developers, 2004
MIUB ECHO-G	Meteorological Institute of the University of Bonn, Meteorological Research Institute of the Korea Meteorological Administration (KMA), and Model and Data Group, Germany/Korea	T30 ($\sim 3.9° \times 3.9°$) L19 Roeckner et al., 1996	$0.5° - 2.8° \times 2.8°$ L20 Wolff et al., 1997
MPI ECHAM5	Max Planck Institute for Meteorology, Germany	T63 ($\sim 1.9° \times 1.9°$) L31 Roeckner et al., 2003	$1.5° \times 1.5°$ L40 Marsland et al., 2003
NCAR CCSM 3.0	National Center for Atmospheric Research, USA	T85 ($1.4° \times 1.4°$) L26 Collins et al., 2004	$0.3° - 1° \times 1°$ L40 Smith and Gent, 2002
UKMO HadCM3	Hadley Centre for Climate Prediction and Research/Met Office, UK	$\sim 1.3° \times 1.9°$ L38 Pope et al., 2000	$0.3° - 1.0° \times 1.0°$ L40 Gordon et al., 2000

Title Page

Abstract | Introduction

Conclusions | References

Tables | Figures

|◄ | ►|

◄ | ►

Back | Close

Full Screen / Esc

Printer-friendly Version

Interactive Discussion
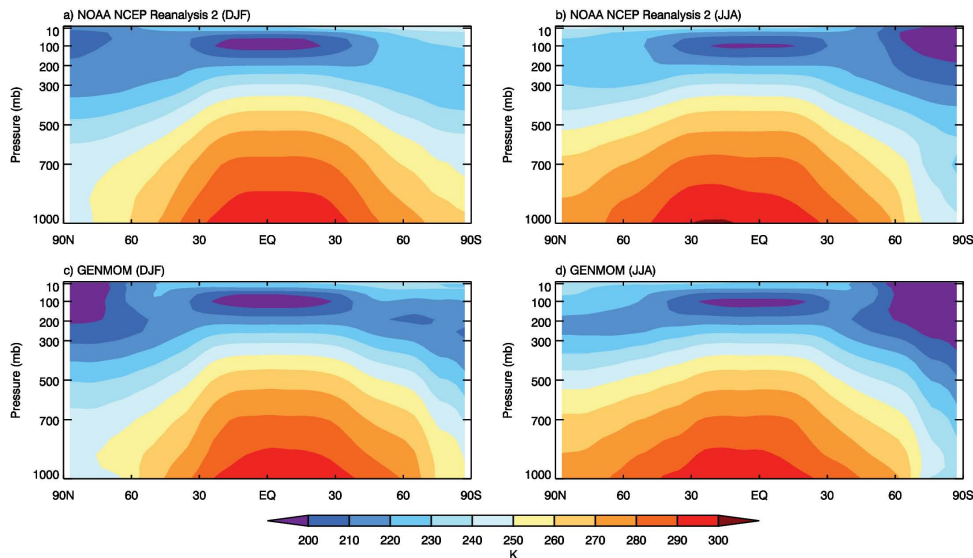
Fig. 1. Mean-annual zonal averaged atmospheric temperature profiles. **(a)** Observed (NCEP2, 1981–2005) December, January, February (DJF), **(b)** Observed June, July, and August (JJA), **(c)** GENMOM DJF, **(d)** GENMOM JJA.
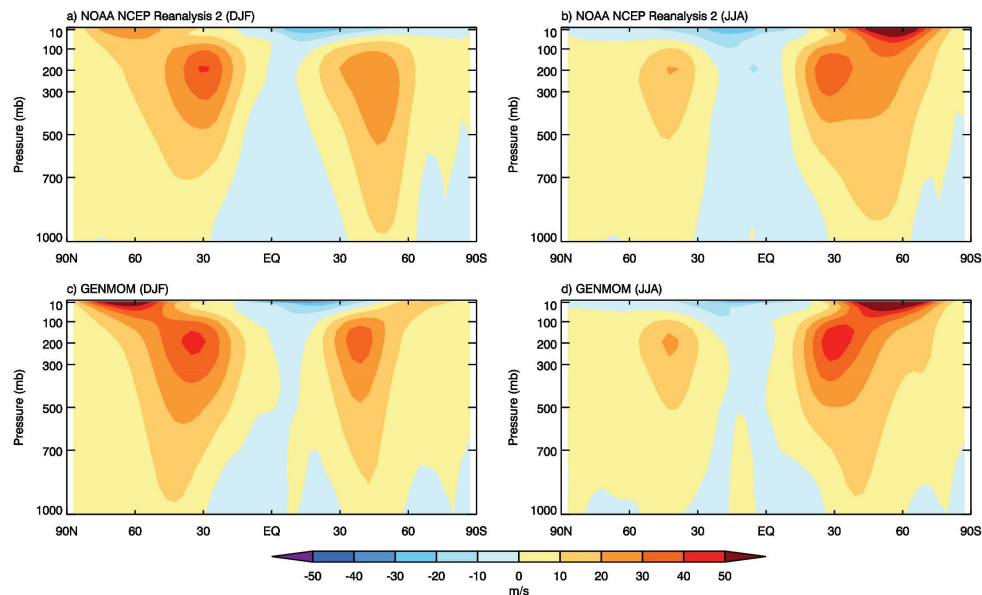
Fig. 2. Winter (DJF) and summer (JJA) zonally averaged eastward wind velocity. **(a)** Observed (NCEP2, 1981–2005) DJF, **(b)** Observed JJA, **(c)** GENMOM DJF, **(d)** GENMOM JJA.
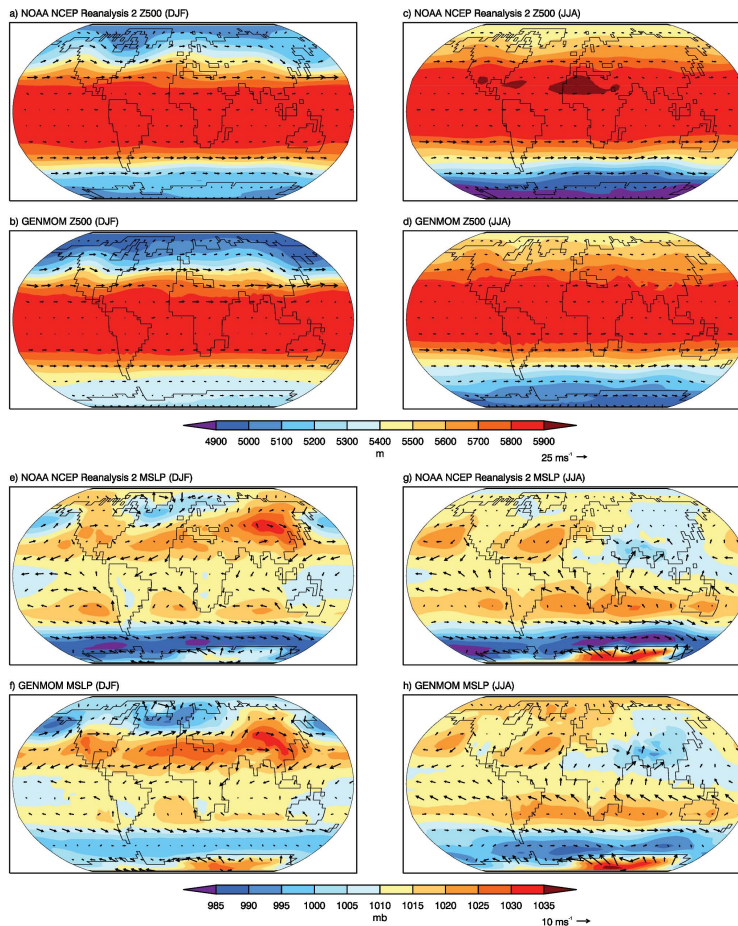
Fig. 3. 500 hPa geopotential height (Z500, **a–d**) and mean sea level pressure (MSLP, **e–h**) with wind vectors for both winter (DJF) and summer (JJA).

Title Page

Abstract   Introduction

Conclusions   References

Tables   Figures

◀   ▶

◀   ▶

Back   Close

Full Screen / Esc

Printer-friendly Version

Interactive Discussion
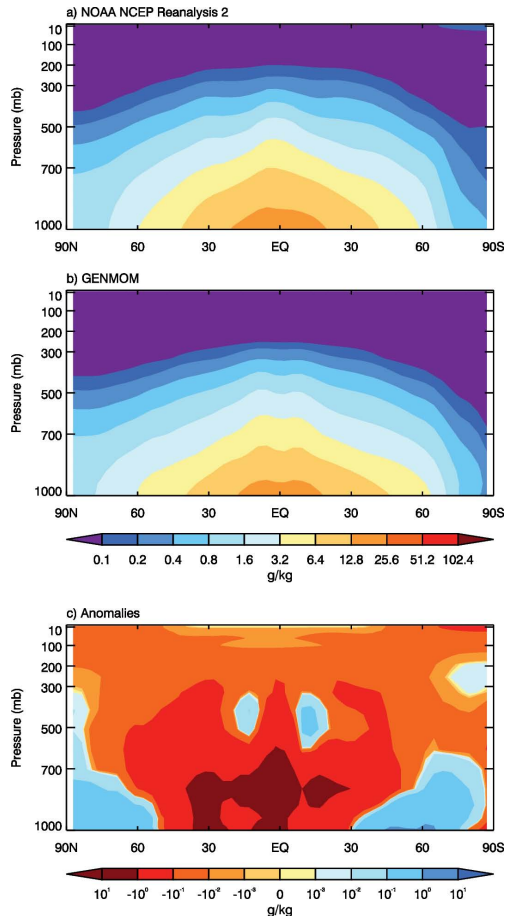
Fig. 4. Mean-annual zonally averaged specific humidity profiles. **(a)** Observed (NCEP2, 1981–2005), **(b)** GENMOM, **(c)** Anomalies are calculated as GENMOM-NCEP2.

Evaluation of a present-day climate simulation

J. R. Alder et al.
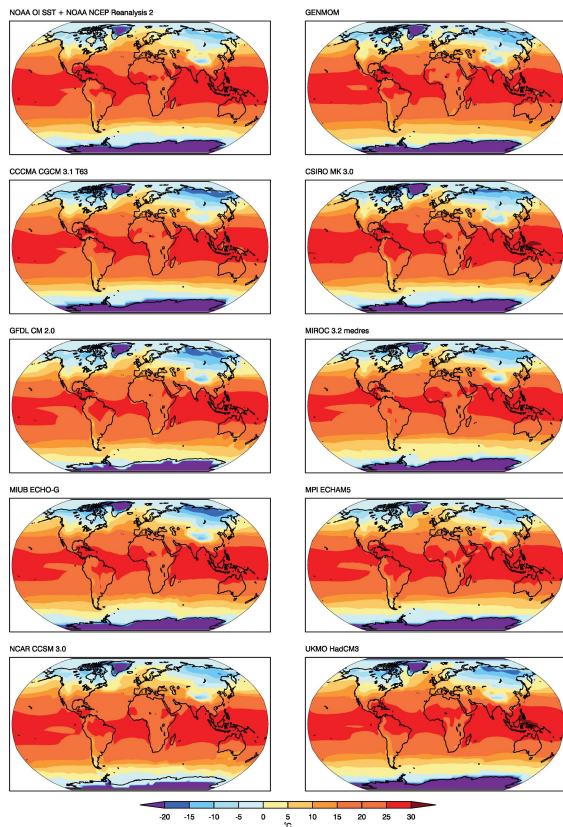
Fig. 5. Observed and simulated annual surface temperature from GENMOM and 8 AOGCMs included in the IPCC AR4. Observed data are from NOAA NCEP Reanalysis 2 (over land) and NOAA OI SST (over sea). GENMOM 2 m air temperature and SST are for model years 670–699 of the control equilibrium simulation. All IPCC AR4 models are averaged over the last 30 years (1970–1999) of the Climate of the 20th Century experiment. All data are bi-linearly interpolated to a 5° × 5° grid.

Full Screen / Esc

Printer-friendly Version

Interactive Discussion
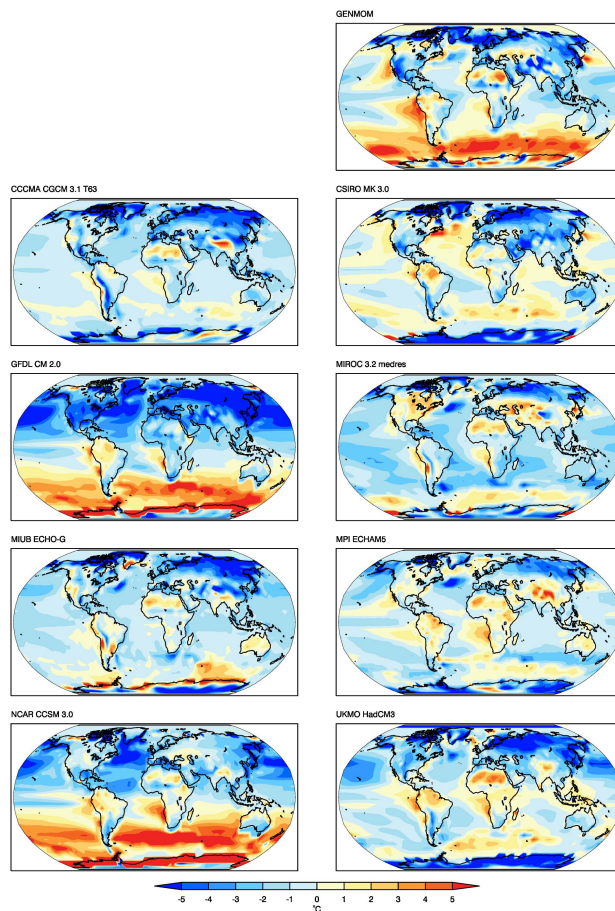
Fig. 6. Anomalies between simulated and observed surface temperatures. Data are described in Fig. 5. Anomalies are calculated as simulation – observation.

Full Screen / Esc

Printer-friendly Version

Interactive Discussion
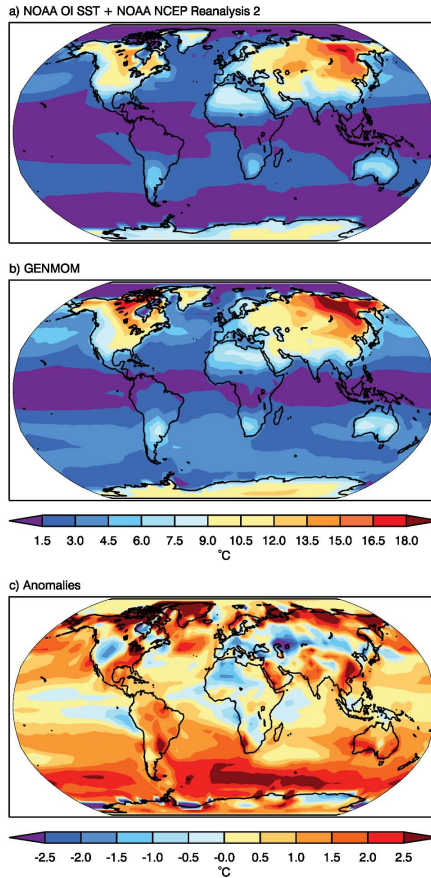
Fig. 7. Observed and modeled seasonal cycle amplitude of surface temperature and anomalies. The amplitude of the seasonal cycle is calculated as the standard deviation of the 12 climatological months.

Full Screen / Esc

Printer-friendly Version

Interactive Discussion
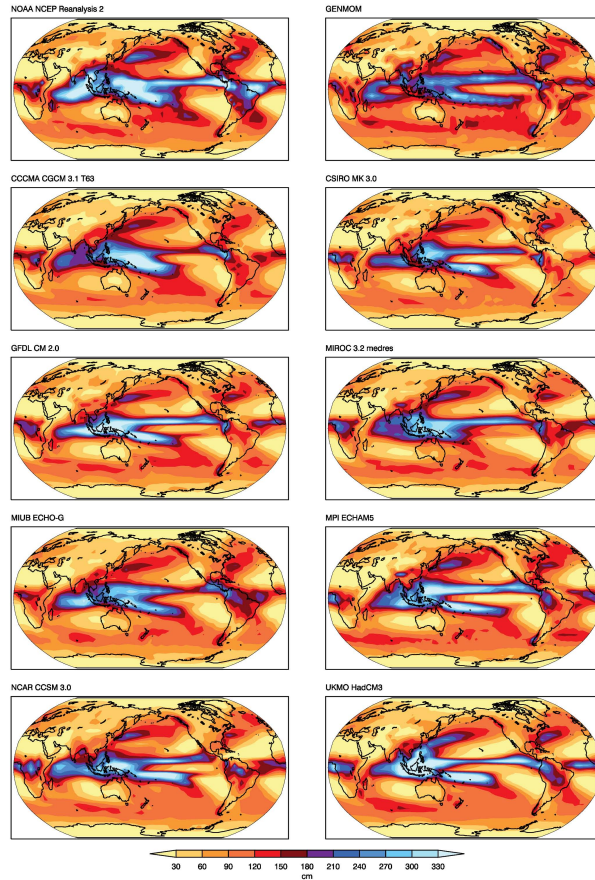
Fig. 8. Observed and simulated mean annual total precipitation from GENMOM and 8 AOGCMs included in IPCC AR4. All IPCC AR4 models are averaged over the last 30 years (1970–1999) of the Climate of the 20th Century experiment. All data are bi-linearly interpolated to a 5° × 5° grid.
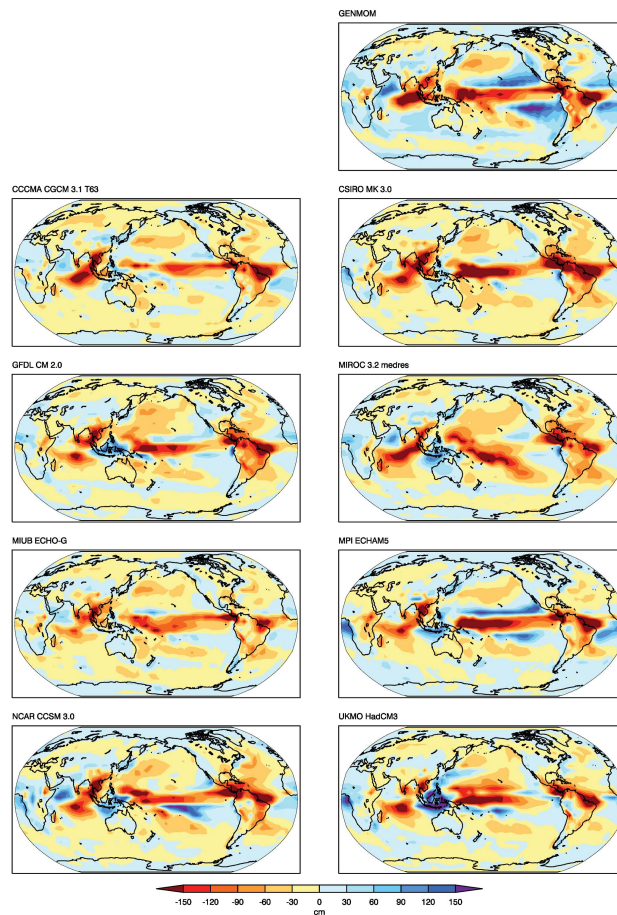
Fig. 9. Anomalies between simulated annual total precipitation and observations. Data are described in Fig. 8. Anomalies are calculated as simulation – observation.

Full Screen / Esc

Printer-friendly Version

Interactive Discussion

Fig. 10. Zonal averaged annual precipitation for observations (black), GENMOM (red) and 8 IPCC AR4 models (gray). All IPCC AR4 models are averaged over the last 30 years (1970–1999) of the Climate of the 20th Century experiment.
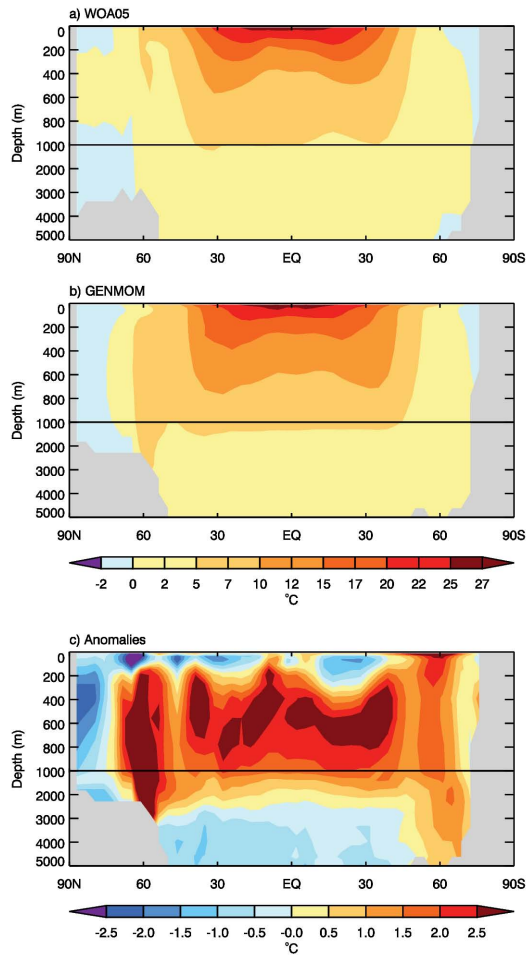
Fig. 11. Mean-annual zonally averaged ocean temperature profile. **(a)** Observed (WOA05), **(b)** GENMOM, **(c)** Anomalies, calculated as GENMOM – observed.

Title Page

Abstract | Introduction

Conclusions | References

Tables | Figures

|◄ | ►|

◄ | ►

Back | Close

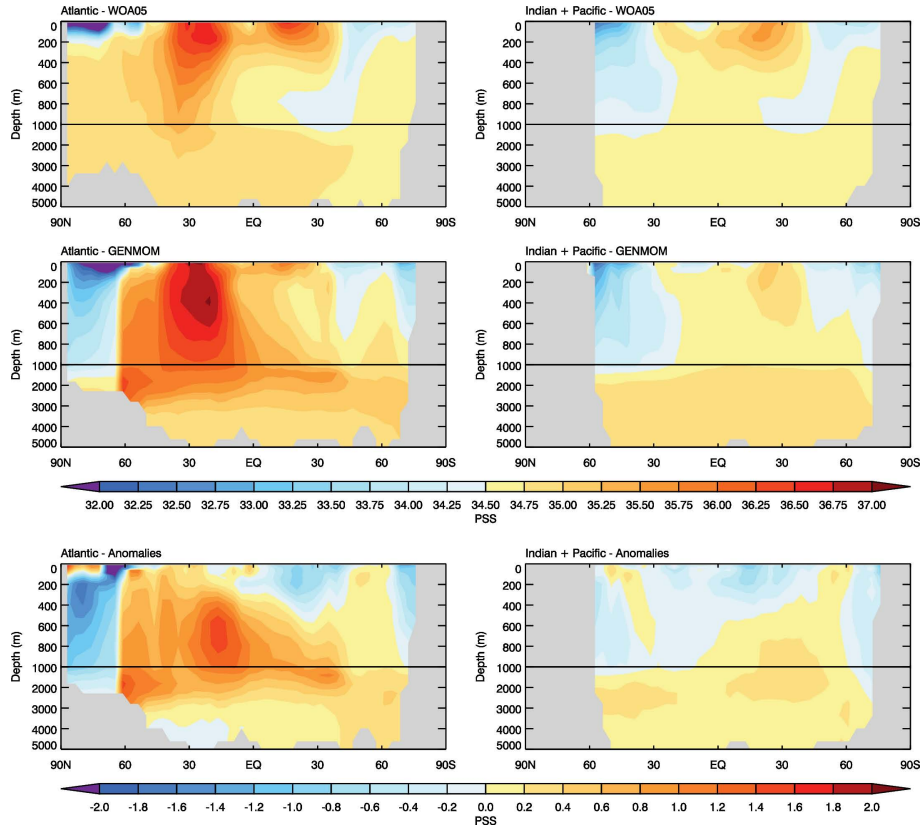Full Screen / Esc

Printer-friendly Version

Interactive Discussion

Fig. 12. Mean-annual zonally averaged ocean salinity profile for both observed (WOA05) and simulated (GENMOM) for the Atlantic Ocean (top), Indian and Pacific Oceans (middle), and anomalies between observed and simulated (bottom).

Title Page

Abstract | Introduction

Conclusions | References

Tables | Figures

|◀ | ▶|

◀ | ▶

Back | Close

Full Screen / Esc

Printer-friendly Version
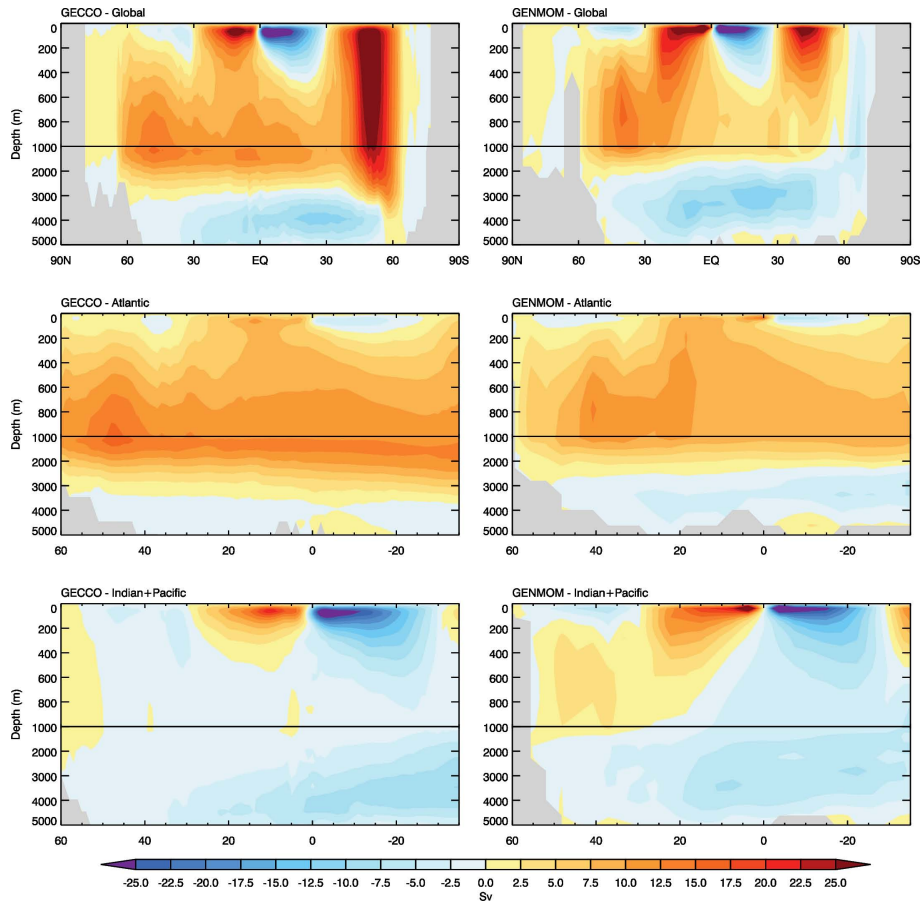
Interactive Discussion

Fig. 13. Ocean overturning for both observed (GECCO) and simulated (GENMOM, full 300-year simulation) globally (top), Atlantic Ocean (middle), Indian and Pacific Oceans (bottom).
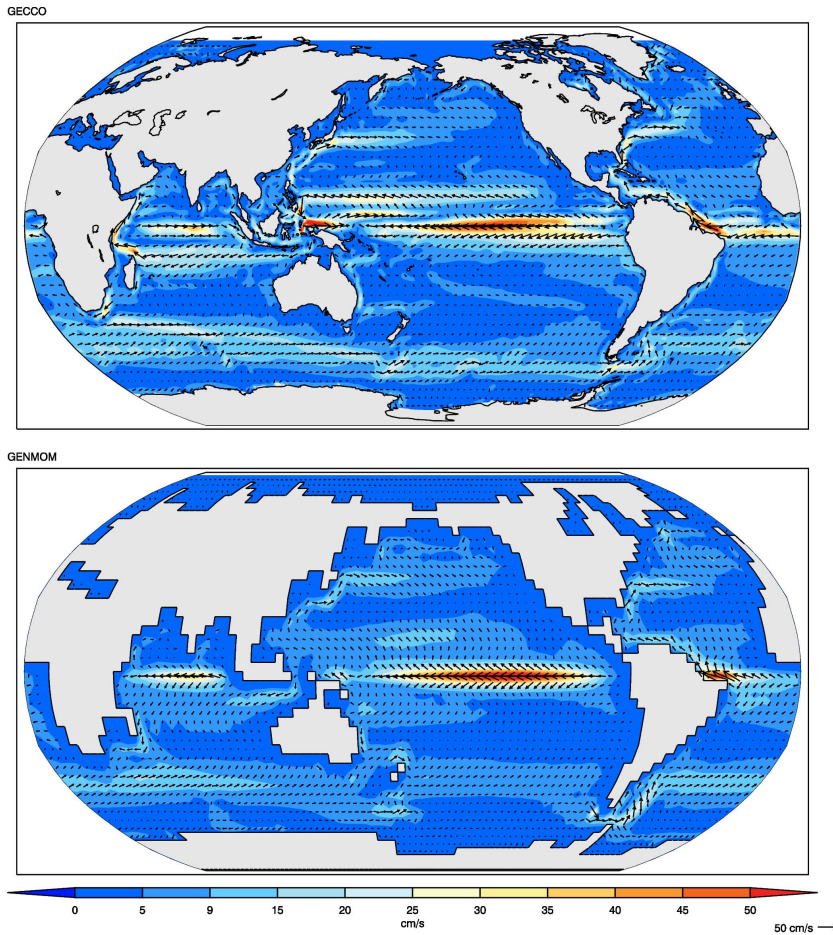
Title Page	
Abstract	Introduction
Conclusions	References
Tables	Figures
◄◄	►►
◄	►
Back	Close
Full Screen / Esc	
Printer-friendly Version	
Interactive Discussion	

Fig. 14. Annual global surface currents for both observations (GECCO) and GENMOM simulated.

Full Screen / Esc

Printer-friendly Version

Interactive Discussion

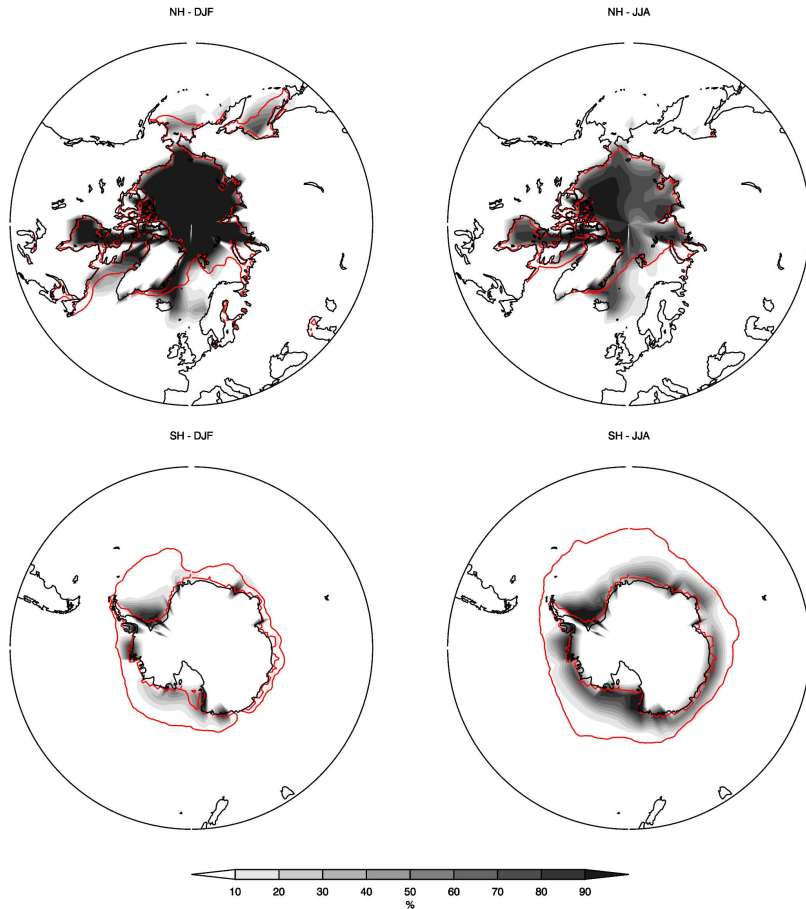Printer-friendly Version

Interactive Discussion

Fig. 15. Fractional sea-ice extent. HadISST v1.1 15% observed contour plotted in red.